Impedance Boundary Conditions on The Optimal Design of the H-Type Cylinder Resonator Using Transmission Matrix Method and Genetic Algorithm

Yosi Aprian SARI
Graduate School, Mathematics and Natural Sciences, Universitas Gadjah Mada, Bulaksumur, Yogyakarta, Indonesia, yosi.aprian.s@mail.ugm.ac.id

Agung Bambang Setio UTOMO
Graduate School, Mathematics and Natural Sciences, Universitas Gadjah Mada, Bulaksumur, Yogyakarta, Indonesia, agungbambang@ugm.ac.id

Mitrayana MITRAYANA
Graduate School, Mathematics and Natural Sciences, Universitas Gadjah Mada, Bulaksumur, Yogyakarta, Indonesia, mitrayana@ugm.ac.id

Danang LELONO
Graduate School, Mathematics and Natural Sciences, Universitas Gadjah Mada, Bulaksumur, Yogyakarta, Indonesia, danang@ugm.ac.id

Abstract: - Optimization of the H-type cylinder resonator design is very important in order to obtain maximum acoustic wave signal in photoacoustic. Geometrically, this resonator is in the form of three cylinders arranged axis-symmetric where the middle cylinder (resonator) is flanked by two other cylinders (buffer) giving sudden contraction and expansion. Impedance boundary conditions are used to analyze the waves propagating in this resonator. The method used in this optimization is the transmission matrix (TM) method and genetic algorithm (GA), in which the transmission loss (TL) at a certain frequency and quality factor (Q_j) are treated as optimization objectives for the cell performance, whereas the resonator geometry dimensions are treated as an optimization.

Keywords: - optimization, H-type cylinder resonator, impedance boundary conditions, transmission matrix method, genetic algorithm

1. INTRODUCTION

A photoacoustic (PA) signal is generally weak and an acoustic resonator is used to amplify the signal. Optimization of the resonator geometry is important to maximize the PA signal. Since the optimal resonator geometry has not been obtained yet, often different shapes of resonators are tested. Experimentally, testing a large number of shapes would be very time consuming and expensive. Therefore, the numerical and/or simulation methods are preferred [1–3].

The most frequently used configuration of the resonator is cylindrical because of its simple symmetry, which coincides with the laser beam propagating along the axis of the cylinder or one of its varieties. The characteristics of cylindrical resonators are longitudinal, azimuth, and radial variations. The problem of acoustic propagation in a cylinder whose cross-sectional area changes suddenly, which is called duct discontinuity is the main problem in this study, both acoustic propagation from cylinders with large to small cross-sectional areas (contraction) or vice versa (expansion). Sudden contractions are widely used in various fields including civil engineering, nuclear engineering, mechanical engineering, chemical engineering, pharmaceutical, food, acoustic, and biomedical. The problem of contraction or expansion has not just become a particular subject but has also been developed in multi-disciplinary engineering approaches such as bio-engineering. For example, a sudden contraction of the vascular network is considered as the flow of a pipe.

Miles [4,5] were the first to investigate the discontinuity problem of acoustic waves in a cylindrical duct. He wrote the fundamental equations governing the propagation of sound near discontinuities and showed that duct discontinuities can be analogous to the impedance. Karal [6] investigated the acoustic inductance for duct discontinuities in two circular ducts of infinite length of various cross-sections, which combine to form an acoustic transmission system. Here, He also stated

that the acoustic pressure passing through the resonator (a duct with a smaller radius) was only valid at very low frequencies. Furthermore, Alfredson [7] developed a method to predict the behavior of wave propagation in a duct whose cross-sectional area varies continuously. Morse and Ingard [8] used a piston approach to study sound radiation into a circular duct taking into account the stopping effect.

Furthermore, Kergomard and Garcia [9] used the mode matching method to obtain the Karal [6] correction factor of the coaxial discontinuity. They have also discussed in great detail the convergence criteria and the amount of mode to be considered for various parameter values. Finally, they provide a set of equations for the case of radiation from a piston plane into an infinite waveguide in the case of a change in circular cross section. Kergomard [10] then developed the method of mode matching and matrix scattering as applied to planar intersections. The developed mode of propagation method for analyzing discontinuities in waveguides is based on a special partition of the impedance matrix. Furthermore, Kemp *et al*. [11] also conveyed what Karal [6] stated but also for higher order mode.

Applications of this duct discontinuity include problems in room acoustics, automotive, and even PAs. Meissner [12] investigated the acoustic resonance frequency in two rooms of different sizes, then Bijen *et al.* [13] and Besson and Thévenaz [14] investigated the shape of the PA resonator in which a large cylindrical cross-sectional area functions as a buffer or damper interference. A similar study is applied in the field of automotive. Selamet and Radavich [15] investigated the effect of the acoustic attenuation performance of concentric expansion chambers using an analytical approach as well as a computational solution based on the boundary element method. Solokhin [16] developed an analytical method for continuous axial pressure and velocity for large sound dampers based on a point-location approach. Furthermore, Homentcovschi and Miles [17] applied the expansion method to analyze axis-symmetric duct discontinuities.

The modeling development in this problem deals with acoustic propagation in three cylindrical tubes, which are combined on one axis in such a way as to form a system called a resonator known as an H-type resonator.

Specifically in the PA field, the design of the H-type cylindrical resonator has been carried out using various methods, e.g.: Duggen *et al.* [18] studied the diameters of the resonator and buffer to obtain the required resonance; Duggen *et al.* [19] used the finite element method to design the geometric shape of the resonator. Yang *et al.* [20] performed a simulation using the four-pole network method; Tavakoli *et al.* [21] used an electrical transmission model corresponding to the resonator cell. Rey *et al.* [22] conducted an experiment to obtain the highest PA signal. Furthermore, Rey and Sigrist [23] conducted experiments with unequal buffer lengths flanking the resonator. Likewise, Bijnen *et al.* [13] used electrical transmission for a first-order longitudinal variation, which theoretically resulted a resonant frequency of 1750 Hz with a radius (r_{res}) and a resonator length (l_{res}) of 3 mm and 100 mm, respectively, and the radius (r_{buf}) and length (l_{buf}) of the buffer are given by $r_{\mathrm{buf}} = 3r_{\mathrm{res}}$ and $l_{\mathrm{buf}} = 50$ mm, respectively. Another result was presented by Mannoor *et al.* [24] who used geometric effects on the performance of H-type cylindrical PA cells using an experimental method design to evaluate the relative impact of cell dimensions on the acoustic response.

In this study, the optimal design of the H-type cylindrical resonator refers to the shape of the resonator according to Bijnen *et al.* [13]. To determine the optimal design value and its resonant frequency, the H-type resonator is analyzed using impedance boundary conditions, transmission matrix (TM) method, and genetic algorithms (GAs). Impedance boundary conditions and TMs are used because they are associated with sudden changes in the cross-sectional area (contraction and expansion) that affect acoustic propagation. The GA method is used because according to Yeh *et al.* [25] it has better accuracy and shorter time than other optimization methods.

2. ACOUSTIC PROPAGATION IN H-TYPE CYLINDER RESONATOR

Acoustic propagation produces convection waveforms. The convection wave equation in the z-direction is [6,26,27]:

$$\nabla^2 p(\vec{r},\omega) + k_0^2 p(\vec{r},\omega) = 0$$
$$\partial p/\partial n = 0 \quad \text{on} \quad \Gamma_1 \cup \Gamma_2 \cup \Gamma_3 \cup \Gamma_4 \cup \Gamma_5 \qquad (1)$$

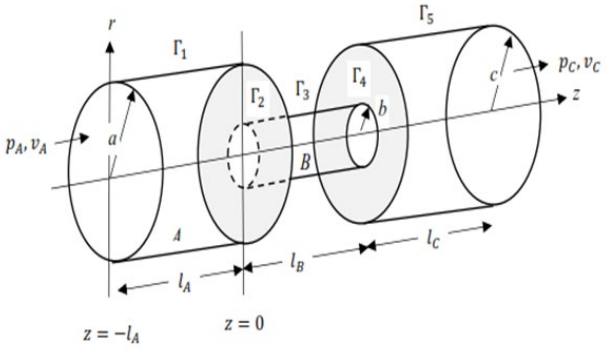

Figure 1. H-type cylinder resonator system.

where $k = \omega/c_s$ is the wave number and c_s is the speed of sound. *A*, *B*, and *C* cylinders are coupled to each other so that the azimuth normal mode form must be orthogonal and axis-symmetric, i.e.: $m = 0$ (see Figure 1).

The general solution of equation (1) relating to the three coupled cylinders is given in Liu *et al.* [28], i.e.:

$$p(r,z) = \begin{cases} \sum_{n=0}^{\infty} \left\{ \begin{bmatrix} A_n^+ e^{ik_{zA}(z+l_A)} + A_n^- e^{-ik_{zA}(z+l_A)} \end{bmatrix} \times J_0\left(\frac{\pi\alpha_{0n}}{a} r\right) \right\}, \\ \begin{cases} -l_A \le z \le 0 \\ 0 \le r \le a \end{cases} \\ \sum_{n'=0}^{\infty} \left\{ \begin{bmatrix} B_{n'}^+ e^{ik_{zB}z} + B_{n'}^- e^{-ik_{zB}z} \end{bmatrix} \times J_0\left(\frac{\pi\alpha_{0n'}}{b} r\right) \right\}, \\ \begin{cases} 0 \le z \le l_B \\ 0 \le r \le b \end{cases} \\ \sum_{n''=0}^{\infty} \left\{ \begin{bmatrix} C_{n''}^+ e^{ik_{zC}(z-l_B)} + C_{n''}^- e^{-ik_{zC}(z-l_B)} \end{bmatrix} \times J_0\left(\frac{\pi\alpha_{0n''}}{c} r\right) \right\}, \\ \begin{cases} l_B \le z \le l_B + l_C \\ 0 \le r \le c \end{cases} \end{cases} \quad (2)$$

Moreover, the speed of the acoustic volume is

$$Q(r,z,\omega) = \frac{-S}{i\omega\rho_0}\frac{dp}{dz} \quad (3)$$

From Figure 1, the boundary conditions of Γ_1 and Γ_2 are the contraction duct discontinuities, whereas Γ_3 and Γ_4 are the expansion duct discontinuities. Γ_5 must meet the boundary condition of $\partial p/\partial n = 0$ and continuous at the discontinuity points of $z = 0$ and $z = l_B$.

Acoustic propagation on sudden changes in the cross section of the cylinder has been studied by Lighthill [29]. The propagated wave undergoes reflection and transmitted only by the impedance mismatch of the plane wave, $\rho_0 c_S/S$, with ρ_0, c_S, and S are the density of the medium, the speed of sound, and the cross section, respectively.

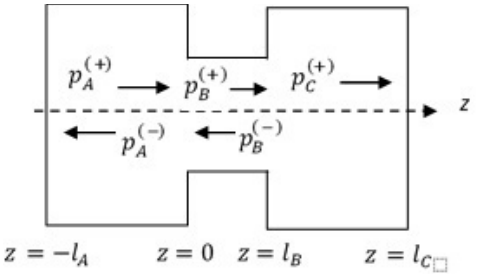

Figure 2. H-type cylindrical resonator acoustic pressure propagation analysis.

Impedance is a very important concept in acoustics [30,31]. On a real surface or solid object, the impedance is determined by the relationship between the acoustic pressure $p(z,\omega)$ and the normal component of the particle's velocity, $v(z,\omega)$. This relationship depends on the angular frequency, ω. Impedance can be used as a boundary condition on the surface of a body, and it is possible to solve the problem of waves outside the body without explicitly addressing the inside of it [32–34], which is given by

$$Z(z,\omega) = \frac{p(z,\omega)}{v(z,\omega)}. \quad (4)$$

The problem can be extended if two or more cylinders are connected through parallel axes with different lengths and cross-sectional areas, so that the impedance and frequency obtained are highly dependent on the parameters of each cylinder. The geometrical problem of the resonator is a very important problem, especially when duct discontinuity is the main problem in this study, both for contraction or expansion.

2.1. Impedance on the H-type Cylinder Resonator

a. Contraction discontinuity

In the propagation of the contraction duct with the boundary conditions $z = -l_A$ and $z = 0$, the impedance is obtained (see Figure 2) as follows [32]:

$$Z_A(0) = Z_{0A}\frac{[iZ_{0A}\tan(k_{zA}l_A) - Z_A(-l_A)]}{[iZ_A(-l_A)\tan(k_{zA}l_A) - Z_{0A}]} \quad (5)$$

where

$$Z_{0A} = \frac{\omega\rho_0}{S_A k_{zA}}.$$

If cylinder *A* is closed at $z = -l_A$ then $Z_A(-l_A) \to \infty$, such that we get

$$Z_A(0) = \frac{iZ_{0A}}{\tan(k_{zA}l_A)}. \quad (6)$$

In the same way for cylinder *B* at $z = 0$ and $z = l_B$, we get

$$Z_B(0) = Z_{0B}\frac{[Z_B(l_B) + iZ_{0B}\tan(k_{zB}l_B)]}{[Z_{0B} + iZ_B(l_B)\tan(k_{zB}l_B)]}, \quad (7)$$

where

$$Z_{0B} = \frac{\omega\rho_0}{S_B k_{zB}}.$$

Cylinders A and B are connected axis-symmetric at $x = 0$. Not all of the incoming waves are transmitted; there are some that are reflected. The first condition that must be met is that on both sides of the discontinuity the pressure is the same, i.e.: $p_A = p_B$. Furthermore, the continuity principle requires that the volume velocity at the duct discontinuity must be the same between the left and right sides, $Q(0^-) = Q(0^+)$, that is, the impedance $Z^{(-)} = p_A/v_A$ and $Z^{(+)} = p_B/v_B$ on both sides of the discontinuity are connected by the equation:

$$\frac{Z_A(0^-)}{S_A} = \frac{Z_B(0^+)}{S_B}. \quad (8)$$

Hence, the impedance of the contraction discontinuity is obtained, viz.:

$$Z_B(l_B) = iZ_{0B}\frac{[S_B S_B k_{zB} - S_A k_{zA} S_A \tan(k_{zA} l_A)\tan(k_{zB} l_B)]}{[S_A S_A k_{zA}\tan(k_{zA} l_A) + S_B S_B k_{zB}\tan(k_{zB} l_B)]}.$$

On the contraction discontinuity, $S_A > S_B$, then the form $S_B k_{zB} S_B \tan(k_{zB} l_B)$ in the denominator of the equation above can be neglected. If we assume that the wavelength of the propagated sound is very small compared to the length of the cylinder, $k_{zA} l_A \ll 1$ and $k_{zB} l_B \ll 1$, then the impedance can be simplified as:

$$Z_B(l_B) = i\omega\rho_0 \frac{\left[S_B - \frac{S_A S_A k_{zA}}{S_B k_{zB}} k_{zA} l_A k_{zB} l_B\right]}{S_A k_{zA} S_A k_{zA} l_A}, \quad (9)$$

which is a direct consequence of the continuity equation. This proves that any sudden change in the cross section of the duct acts as an impedance transformer.

b. Expansion discontinuity

As in cylinder A, if cylinder C is closed at $z = l_B + l_C$, then $Z(l_B + l_C) \to \infty$ and because of the discontinuity of the ducts of cylinders B and C, $S_B < S_C$ is a form of expansion, and assuming that $k_{zC} l_C \ll 1$ then the equation for the impedance of cylinders B and C becomes:

$$Z_C(l_B) = \frac{-iZ_{0C}}{k_{zC} l_C}. \quad (10)$$

If the discontinuity of AB duct is connected to cylinder C and has a discontinuity point at $z = l_B$, then:

$$\frac{Z_B(l_B^-)}{S_B} = \frac{Z_C(l_B^+)}{S_C}. \quad (11)$$

By substituting equations (9) and (10) into equation (11) and assuming the dimensions of cylinders A and C are the same, then the longitudinal wave number is obtained as follows:

$$k_{zC}^2 = k_{zA}^2 = \frac{S_B^2}{l_A l_B S_A^2} \quad (12)$$

and the wave number in cylinder B (resonator) has been known previously [14], that is:

$$k_{zB}^2 = \left(\frac{\pi k}{l_B}\right)^2 = k_0^2 - \left(\frac{\pi\alpha_{mn}}{b}\right)^2. \quad (13)$$

Thus, the resonant frequency of the H-type cylinder resonator can be obtained by the sum of wave numbers of each cylinder, and assuming $S_A = S_C$, we have [35]:

$$k_0^2 = k_{zA}^2 + k_{zB}^2 + k_{zC}^2$$

that is

$$\omega_{kmn} = c_s\sqrt{\frac{2S_B^2}{l_A l_B S_A^2} + \left(\frac{\pi k}{l_B}\right)^2 + \left(\frac{\pi\alpha_{mn}}{b}\right)^2} \quad (14)$$

where k, m, and n are the longitudinal, azimuthal, and radial normal modes, respectively; c_s, b, S_A, S_B, l_A, l_B, and α_{mn} are the speed of sound in the medium, the radius of cylinder B, the cross-sectional areas of cylinders A and B, the lengths of cylinders A and B, and the n^{th} root of the equation involving the m^{th} order Bessel function, respectively.

The wave number in equation (12) is a combination of the dimensions of cylinder A (buffer) and cylinder B (resonator), which shows that the impedance at the duct discontinuity of the resonator vanishes at a certain resonant frequency, which is the correction factor for the single cylinder resonant frequency in equation (13).

2.2 Transmission Matrix (TM) Method and Transmission Loss (TL)

The next method used is the TM method, which is based on the principle of the acoustic behavior of

plane waves on a uniform tube element with a length L, in which the fluid flows uniformly (average density ρ_0 and speed of sound c_S). The transmission of acoustic pressure from point $z = -l_A$ to point $z = l_B + l_C$ that passes through the duct discontinuity is in the form of a sudden change in cross-sectional area both contraction ($z = 0$) and expansion ($z = l_B$). With a certain length of the duct, this causes the propagating wave to change as a function of these parameters. The important aspect in this assumption is that the wave propagates linearly, adiabatically, and without any loss due to wave propagation. Here, the propagation is in the smallest longitudinal mode ($n = 0$), meaning that the pressure (p) and volume velocity (Q) do not change as they pass through the duct discontinuity. The boundary conditions at the discontinuity duct are as follows: the continuity of the pressure and axial particle velocity on the $z = 0$ and $z = l_B$ can be written as:

$$\left.\begin{aligned} p(0^-) &= p(0^+) \\ p(l_B^-) &= p(l_B^+) \end{aligned}\right\}, 0 \le r < b$$
$$\left.\begin{aligned} Q(0^-) &= Q(0^+) \\ Q(l_B^-) &= Q(l_B^+) \end{aligned}\right\}, 0 \le r < b$$
$$Q(0^+) = 0, \qquad b \le r \le a$$
$$Q(l_B^-) = 0. \qquad b \le r \le c \tag{15}$$

From this assumption, and from equations (2) and (3) as well as the analysis of Figure 2, the wave transmission can be described as follows:

(i) Pressure and volume velocity at $z = 0$

$$A^+ e^{ik_{zA}l_A} + A^- e^{-ik_{zA}l_A} = B^+ + B^-, \tag{16a}$$

and

$$S_A k_{zA}\left[A^+ e^{ik_{zA}l_A} - A^- e^{-ik_{zA}l_A}\right] = S_B k_{zB}[B^+ - B^-], \tag{16b}$$

by eliminating the shape of the reflection ($-$), we get the relationship:

$$\left(1 + \frac{S_B k_{zB}}{S_A k_{zA}}\right) B^+ + \left(1 - \frac{S_B k_{zB}}{S_A k_{zA}}\right) B^- = 2A^+ \cos(k_{zA}l_A). \tag{17}$$

(ii) Continuous pressure and volume velocity at a discontinuity of $z = l_B$

$$B^+ e^{ik_{zB}l_B} + B^- e^{-ik_{zB}l_B} = C^+, \tag{18a}$$

and

$$\frac{S_B k_{zB}}{\rho_0 \omega}\left(B^+ e^{ik_{zB}l_B} - B^- e^{-ik_{zB}l_B}\right) = \frac{S_C k_{zC}}{\rho_0 \omega} C^+. \tag{18b}$$

Equation (18a) is substituted into equation (18b), hence we get the incident wave coefficient, B^+, and the transmitted coefficient, C^+, at this discontinuity, i.e.:

$$B^+ = \frac{1}{2}\left[1 + \frac{S_C k_{zC}}{S_B k_{zB}}\right] e^{-ik_{zB}l_B} C^+. \tag{19}$$

In cylinder C, it is assumed that there are no reflected waves such that all waves are transmitted. By substituting equations (18a) and (18b) into equation (17), we get the acoustic waves transmission of the type-H cylinder resonator as:

$$T_{ABC} = \frac{C^+}{A^+} = \frac{2\cos(k_{zA}l_A)}{\left[\cos(k_{zB}l_B)\left(1 + \frac{S_C k_{zC}}{S_B k_{zB}}\frac{S_B k_{zB}}{S_A k_{zA}}\right) - i\sin(k_{zB}l_B)\left(\frac{S_B k_{zB}}{S_A k_{zA}} + \frac{S_C k_{zC}}{S_B k_{zB}}\right)\right]}. \tag{20}$$

If it is assumed that cylinder A has the same dimensions as cylinder C, $S_A k_{zA} = S_C k_{zC}$, then equation (20) becomes simpler, i.e.:

$$T_{ABC} = \frac{2\cos(k_{zA}l_A)}{\left[2\cos(k_{zB}l_B) - i\left(\frac{S_B k_{zB}}{S_A k_{zA}} + \frac{S_A k_{zA}}{S_B k_{zB}}\right)\sin(k_{zB}l_B)\right]}, \tag{21}$$

or the modulus of transmission coefficient is obtained as:

$$|T|^2 = TT^* = \frac{\cos^2(k_{zA}l_A)}{\left[1 + \frac{1}{4}\left(\frac{S_B k_{zB}}{S_A k_{zA}} - \frac{S_A k_{zA}}{S_B k_{zB}}\right)^2 \sin^2(k_{zB}l_B)\right]}, \tag{22}$$

where S_A, S_B, l_A, l_B, k_{zA} and k_{zB} are the cross-sectional areas, the lengths, and the longitudinal wave numbers of cylinders A and B, respectively. The interesting fact here is that the transmitted and reflected waves are related to the cross-sectional area and length of the two cylinders.

From equation (22) the TL may be obtained, which shows the strength of the incident wave that is lost when passing through the duct that function as a damper. In this case, the dampers are cylinders A and C, which have larger sizes than cylinder B, which is

known as the resonator. Therefore, TL is expressed as:

$$\mathrm{TL} = 10\log_{10}\frac{1}{|T|^2}. \quad (23)$$

From equation (20), the TL can be obtained as:

$$\mathrm{TL} = 10\log_{10}\frac{\left[1+\frac{1}{4}\sin^2(k_{zB}l_B)\left(\frac{S_Bk_{zB}}{S_Ak_{zA}}-\frac{S_Ak_{zA}}{S_Bk_{zB}}\right)^2\right]}{\cos^2(k_{zA}l_A)}. \quad (24)$$

There are at least three main criteria to consider in using this method. First, there is noise reduction (NR), insertion loss (IL), and TL. In this problem, TL is used because it takes into account the effect of changes in latitude when propagation occurs and also TL does not depend on the sound source. As long as acoustic propagation occurs, it is assumed that there is no change in pressure and volume velocity in the duct and in the duct discontinuity from source inlet to outlet [36].

2.3 Loss Mechanism and Quality Factor

The geometric shape of the H-type cylindrical resonator has a sudden change in cross-sectional area, which greatly affects the energy of the propagating wave. According to Besson and Thévenaz [14], one of the losses that arise is due to the waves hitting the duct walls, in addition to the viscous and thermal dissipation effects on the duct surface. This loss can be corrected by including the loss factor Q_j.

The value of Q_j is generally a loss by heat conduction and fluid viscosity. Acoustic losses caused by heat conduction and gas viscosity are divided into two, namely volume and surface losses. The surface loss occurs in a thin layer near the wall, which extends to a viscous effect with a thickness $d_{\eta,j}$, and a conduction effect with a thickness $d_{th,j}$. The value of Q_j has been obtained by Besson and Thévenaz [14], which contains the surface and volume loss factors, i.e.:

$$\frac{1}{Q_j} = \frac{1}{Q_{surf}} + \frac{1}{Q_{vol}}, \quad (25)$$

where

$$\frac{1}{Q_{surf}} = \frac{d_{\eta,j} + (\gamma-1)d_{th,j}\left(1+\frac{2b}{l_{res}}\right)}{b}, \quad (26)$$

and

$$\frac{1}{Q_{vol}} = \frac{\omega_j}{2c_s^2}\left[\frac{4}{3}\frac{\eta}{\rho_0} + (\gamma-1)\frac{\kappa}{\rho_0 C_p}\right], \quad (27)$$

where

$$d_{\eta,j} = \sqrt{\frac{2\eta}{\rho_0\omega_j}}, \quad (28)$$

and

$$d_{th,j} = \sqrt{\frac{2KM}{\rho_0\omega_j C_p}}, \quad (29)$$

where η, ρ_0, ω_j, K, M, and C_p, are the viscosity, density of the gas, angular resonant frequency, gas thermal conductivity, molar mass of the gas, and heat capacity at constant pressure, respectively.

3. GENETIC ALGORITHMS (GAs)

The concept of GAs–was first formalized by Holland (1975) and extended to functional optimization by Jong (1975). Later on, the GAs involved the use of optimization search strategies after the Darwinian notion of natural selection and evolution [37]. The GA accomplishes the task of optimization by starting with a random “population" of values for the parameters of an optimization problem. Thereafter, a new “generation" with improved values of the objective function is then produced. In order to achieve evolution in the new generation, the binary system is used. The binary system is a representation of real numbers and integers. In addition, by manipulating the strings, the operators of reproduction, crossover, mutation, and elitism are thus at work sequentially. A brief description of GA operators and their components is as follows [25,38–41]:

a. Populations and Chromosomes: The initial population begins by randomization. The parameter set is encoded to form a string representing the chromosome. By evaluation of the objective function, each chromosome is assigned fitness.
b. Parent: Using the probabilistic computation weighted by the relative fitness, pairs of chromosome are selected as parents. Each individual in the population is assigned a space on the roulette wheel proportional to individual relative fitness. Individuals with the largest

portion on the wheel have the greatest probability of being selected as the parent generation for the next generation.

c. Offspring: One pair of offspring is generated from the selected parent by crossover. Crossover occurs with a probability of pc. Then, random selection is done from the crossover and combination from 2 oldest genetic data. The scheme of single-point crossover is chosen from the GA optimization. Recombination and parent selection are the principle methods for the evolution of the GA.
d. Mutation: This operator is used to provide the needed diversity in the population and to search in different areas. Genetically, mutation occurs with a probability of pm where the new and unexpected points are brought into the GA optimizer's search domain. This is an essential operator that introduces diversity into the population and prevents the GA from becoming saturated with solutions at the local optimum.
e. Elitism: Elitism reintroduces the best candidate in each generation. It can prevent the best gene from disappearing and improves the accuracy of optimization during reproduction.
f. New Generation: Reproduction includes selection, crossover, mutation, and elitism. The reduplication continues until a new generation is constructed and the original generation is substituted. Highly fit characteristics produce more copies of themselves in subsequent generations, resulting in a movement of the population towards an optimal direction. The process can be terminated when the number of predetermined maximum generations (gen_no) has been reached.

The GA method starts by generating random numbers from 0 to 1 in the form of a matrix, which is then converted into binary numbers 0 and 1 (by rounding to 0 if < 0.5 and to 1 if > 0.5). This stored binary number is called population initiation. The next step is the evolution process that starts with decoding the chromosomes into a fitness function that produces a fitness value. This fitness value is processed to get the desired output variable values. Next, the code is converted back to the binary chromosome called encoding. The next step is to sort each individual in the population according to its fitness.

The evaluation process is the main process in this optimization. This process is a bridge between the physical phenomena and the program created. After the evaluation process, the binary chromosomes from the encoding results are matched, such that they reach optimization (threshold). If not achieved, then the next step is the reproduction process. Reproduction is

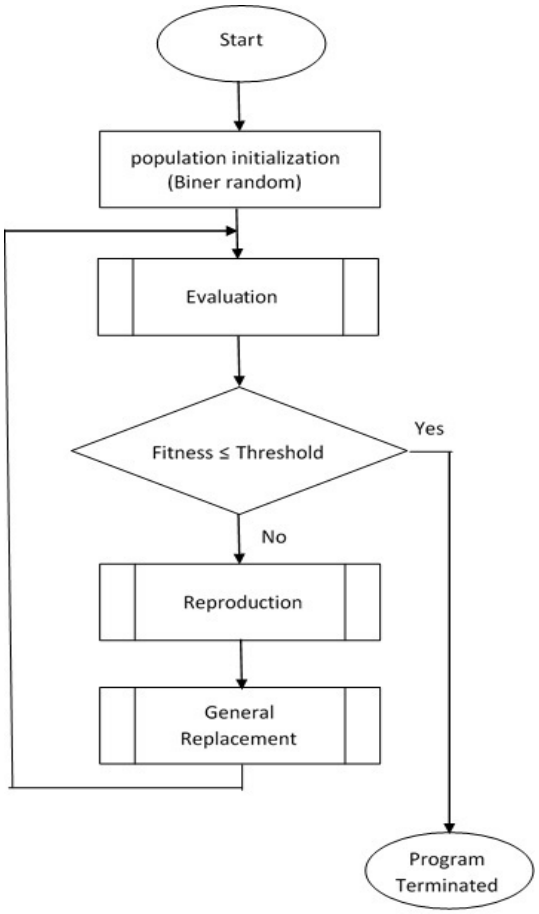

Figure 3. Main Program of GA

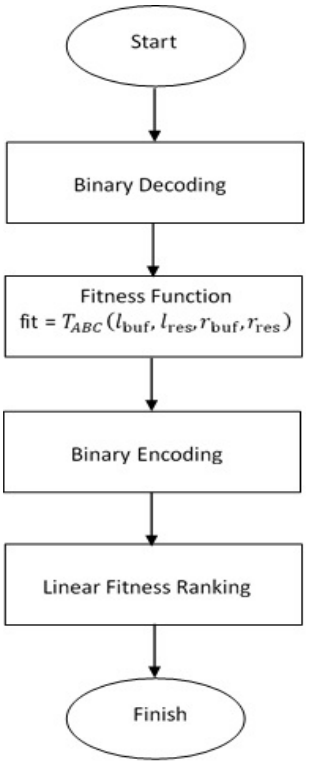

Figure 4. Sub-program of Evaluation

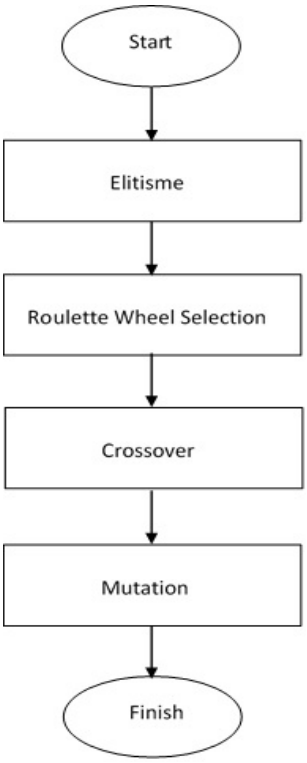

Figure 5. Sub-program of Reproduction

the most important part of the biological process to get a better generation. The first step is to copy the best chromosomes from each population, which is called elitism. Next is the process of selecting parents using a roulette wheel selection, in which the two selected parents will be mated. The mating is carried out by crossing one point of intersection, which produces two different offsprings. The reproduction process will still be on going and some genes in the offspring's chromosomes undergo mutations.

The next process is to completely replace the old generation with the new generation. The new generation from the general replacement results is re-evaluated until the process is stopped if optimization is achieved or until the last generation is processed. The flowchart of the GA for the analysis of the H-type resonator optimization is given in Figure 3.

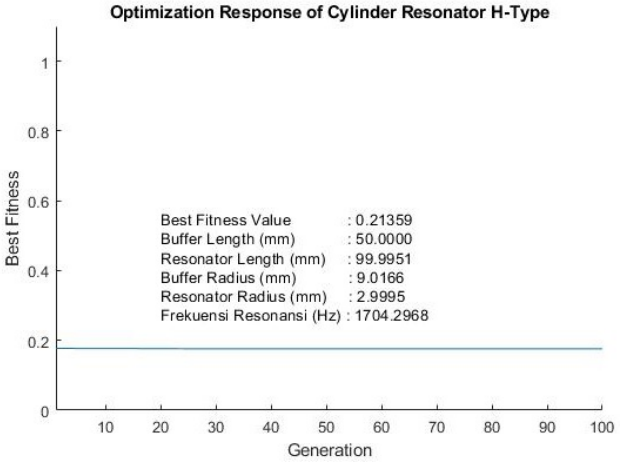

Figure 6. Optimization response of the H-type cylinder resonator

In this study, the optimization of the H-type cylindrical resonator design contains parameters to be optimized, namely the l_{buf} and l_{res} as well as the r_{buf} and r_{res}. In addition, the parameters used in this optimization are c; density of CO_2; number of initial population (pop); probability of crossover (pc); probability of mutation (pm); maximum generation (itermax); and the tolerance value (toll) with values of 340 m/s; 1.98 kg/m^3; 30; 0.95; 0.005; 100; and 10^{-20}, respectively. The fitness response to the maximum generation is shown in Figure 4.

Table 3. Optimization results of GA on the H-type cylinder resonator for the pure longitudinal mode.

No	l_{buf} (mm)	l_{res} (mm)	r_{buf} (mm)	r_{res} (mm)	TL (dB)
1.	50.000	99.995	9.064	3.000	13.590
2.	50.000	99.995	9.003	3.000	17.623
3.	50.005	99.995	9.002	3.000	19.847
4.	50.000	99.995	9.008	3.000	20.590
5.	50.000	99.995	9.017	3.000	12.325

The optimization results in Table 3 show various dimensions of the buffer and resonator and the same resonant frequency, which is 1704.297 Hz on the pure longitudinal modes ($k = 1, m = n = 0$).

Figure 7 shows TL in the cylindrical resonator related to the strength of the incident wave that is lost as it passes through the duct. From Table 3, it may be observed that although the changes in the buffer and resonator dimensions are very small (or even exactly the same) and having the same resonant frequency, the transmission coefficients and TLs are not necessarily the same. The configuration of the buffer and resonator dimensions greatly affects the transmission and acoustic losses. In this study, the largest transmission coefficient value and the smallest TL is expected. This is obtained at l_{buf} of 50.000 mm, r_{buf} of 9.017 mm, l_{res} of 99.995 mm, and r_{res} of 3.000 mm. The results of this optimization are similar to [13], but the frequency is different.

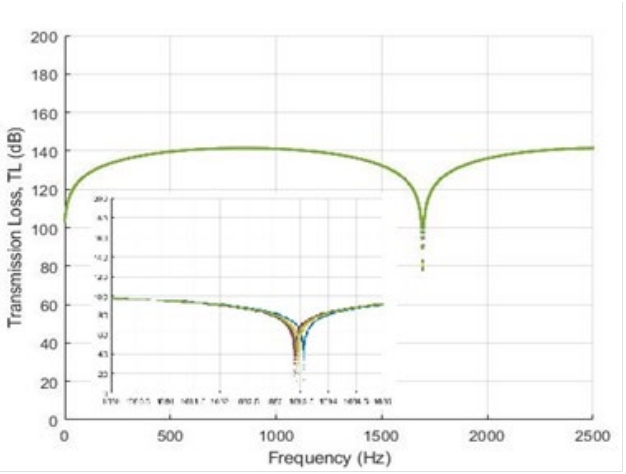

Figure 7. Transmission loss of the H-type cylinder resonator

Furthermore, the value of Q_j associated with the performance of this resonator is $Q_j = 56.239$. The Q_j decreases with increasing l_{res}, which is expected because the Q_j is inversely proportional to the square root of the l_{res}. The Q_j decreases with increasing l_{buf}. As the length increases, the increase in the surface losses dominate the net energy stored in the volume, which results in a lower Q_j.

A limitation of this study is that the pressure and velocity of the acoustic volume before and after passing through the duct discontinuity are the same. To obtain more accurate results, it is necessary to consider the effect of head loss and edge effect on the discontinuity of the duct, thus affecting the pressure and velocity of the volume that propagates in the discontinuity of the duct. In this case, the finite element method can be used because it deals with the effect of boundary conditions [42].

4. CONCLUSION

The configuration of buffer and resonator sizes in wave propagation across duct discontinuities results in varying TL values. The propagating wave loss in its transmission is caused by a sudden change in the cross-sectional area causing the transmitted and reflected waves.

The optimization of the H-type cylindrical resonator design is carried out by considering the impedance limit conditions and using the TM and GA methods. The geometric shape of the H-type resonator has a sudden contraction and expansion, which greatly affects the energy of the acoustic wave propagation. The GA method is used in this optimization to maximize the acoustic transmission coefficient (while minimizing TL) at a certain frequency which is limited by the size of the buffer and resonator, as well as the quality factor Q_j caused by heat conduction and gas viscosity. The results obtained in the pure longitudinal mode of this optimization are 50.000 mm l_{buf}, 9.017 mm r_{buf}, 99.995 mm l_{res}, 3.000 mm r_{res}, the f of 1704.297 Hz, TL of 12.325 dB, and Q_j of 56.239.

ACKNOWLEDGMENTS

The authors would like to thank *Lembaga Pengelola Dana Pendidikan* (LPDP) in providing the funding for this research in the form of LPDP Scholarship with contract number of 201710210211540.

REFERENCES

[1] Baumann B., Kost B., Wolff M., and Groning H., Modeling and Numerical Investigation of Photoacoustic Resonators, *Model. Simul.*, 2008.

[2] El-Busaidy S. A. S., Baumann B., Wolff M., and Duggen L., Modelling of open photoacoustic resonators, *Photoacoustics*, vol. 18, no. September 2019, 2020.

[3] Kost B., Baumann B., Germer M., and Wolff M., Shape optimization of photoacoustic resonators, *WIT Trans. Built Environ.*, vol. 106, no. May, pp. 45–54, 2009.

[4] Miles J. W., The Analysis of Plane Discontinuities in Cylindrical Tubes. Part I, *J. Acoust. Soc. Am.*, vol. 17, no. 3, pp. 259–271, 1946.

[5] Miles J. W., The Analysis of Plane Discontinuities in Cylindrical Tubes. Part II, *J. Acoust. Soc. Am.*, vol. 17, no. 3, pp. 271–284, 1946.

[6] Karal F. C., The Analogous Acoustical Impedance for Discontinuities and Constrictions of Circular Cross Section, *J. Acoust. Soc. Am.*, vol. 25, no. 2, pp. 233–237, 1953.

[7] Alfredson R. J., The Propagation of Sound in a Circular Duct of Continuously Varying Cross-Sectional Area, *J. Sound Vib.*, vol. 23, no. 4, pp. 433–442, 1972.

[8] Morse P. M. and Ingard K. U., *Theoretical Acoustics*. 1986.

[9] Kergomard J. and Garcia A., Simple discontinuities in acoustic waveguides at low frequencies: Critical analysis and formulae, *J. Sound Vib.*, vol. 114, no. 3, pp. 465–479, 1987.

[10] Kergomard J., Calculation of discontinuities in waveguides using mode-matching method: an alternative to the scattering matrix approach, *J. Acoustique*, vol. 4, 1991, pp. 111-138.

[11] Kemp J., Lopez-Carromero A., and Campbell M., Pressure fields in the vicinity of brass musical instrument bells measured using a two-dimensional grid array and comparison with multimodal models, *24th Int. Congr. Sound Vib. ICSV 2017*, 2017.

[12] Meissner M., Effect of cross-sectional area discontinuities in closed hard-walled ducts on frequency of longitudinal modes, *Arch. Acoust.*, vol. 35, no. 3, pp. 421–435, 2010.

[13] Bijnen F. G. C., Reuss J., and Harren F. J. M., Geometrical optimization of a longitudinal resonant photoacoustic cell for sensitive and fast trace gas detection, *Rev. Sci. Instrum.*, vol. 67, no. 8, pp. 2914–2923, 1996.

[14] Besson J. P. and Thévenaz L., Photoacoustic spectroscopy for multi-gas sensing using near infrared lasers, *Lab. nanophotonique métrologie*, vol. Ph.D., no. Thèse No. 3670, 2006, pp. 1–189.

[15] Selamet A. and Radavich P. M., The effect of length on the acoustic attenuation performance of concentric expansion chambers: An analytical, computational and experimental investigation, *J. Sound Vib.*, vol. 201, no. 4, pp. 407–426, 1997.

[16] Solokhin N., Basic types of discontinuity in circular acoustic wave guide, *J. Acoust. Soc. Am.*, vol. 114, no. 5, p. 2626, 2003.

[17] Homentcovschi D. and Miles R. N., Re-expansion method for circular waveguide discontinuities: Application to concentric expansion chambers, *J. Acoust. Soc. Am.*, vol. 131, no. 2, pp. 1158–1171, 2012.

[18] Duggen L., Frese R., and Willatzen M., FEM analysis of cylindrical resonant photoacoustic cells, *J. Phys. Conf. Ser.*, vol. 214, 2010.

[19] Duggen L., Albu M., Willatzen M., and Rubahn H.-G., Modeling frequency response of photoacoustic cells using FEM for determination of N-heptane contamination in air: Experimental validation, *IMETI 2011 - 4th Int. Multi-Conference Eng. Technol. Innov. Proc.*, vol. 2, no. 2, pp. 108–110, 2011.

[20] Yang C., Arsad N., Min L., and Yao W., Buffer structure optimization of the photoacoustic cell for trace gas detection ∗, *optoelectronicsletters*, vol. 9, no. 3, pp. 2–6, 2013.

[21] Tavakoli M., Tavakoli A., Taheri M., and Saghafifar H., Design, simulation and structural optimization of a longitudinal acoustic resonator for trace gas detection using laser photoacoustic spectroscopy (LPAS), *Opt. Laser Technol.*, vol. 42, no. 5, pp. 828–838, 2010.

[22] Rey J. M., Marinov D., Vogler D. E., and Sigrist M. W., Investigation and optimisation of a multipass resonant photoacoustic cell at high absorption levels, vol. 266, pp. 261–266, 2005.

[23] Rey J. M. and Sigrist M. W., Differential mode excitation photoacoustic spectroscopy : A new photoacoustic detection scheme Differential mode excitation photoacoustic spectroscopy : A new photoacoustic detection scheme, vol. 063104, no. 2007, 2012.

[24] Mannoor M., Hwang J., and Kang S., Numerical study of geometrical effects on the performance of an H-type cylindrical resonant photoacoustic cell, *J. Mech. Sci. Technol.*, vol. 32, no. 12, pp. 5671–5683, 2018.

[25] Yeh L. J., Chang Y. C., and Chiu M. C., Shape optimal design on double-chamber mufflers using simulated annealing and a genetic algorithm, *Turkish J. Eng. Environ. Sci.*, vol. 29, no. 4, pp. 207–224, 2005.

[26] Peat K. S., The acoustical impedance at discontinuities of ducts in the presence of a mean flow, *J. Sound Vib.*, vol. 127, no. 1, pp. 123–132, 1988.
[27] Sari R. Y. A., Bambang A., Mitrayana, and Lelono D., Pengaruh Konfigurasi Geometri Buffer Resonator Tipe-H Terhadap Intensitas Bunyi, *J. Sains Dasar*, vol. 9, no. 1, pp. 30–36, 2020.
[28] Liu B., Liu J., Wei W., Shen H., and Wei Z., Suppression of low frequency sound transmission in fluid-filled pipe systems through installation of an anechoic node array, *AIP Adv.*, vol. 8, no. 11, 2018.
[29] Lighthill J., *Waves in fluids*. Cambridge University Press, 1978.
[30] Kinsler L. E., Frey A. R., Coppens A. B., and Sanders J. V., *Fundamentals of Acoustics*, 4 th. 2000.
[31] Noreland D., Impedance boundary conditions for acoustic waves in a duct with a step discontinuity, *Comput. Methods Appl. Mech. Eng.*, vol. 71, no. 2, pp. 197–224, 2003.
[32] Kuttruff H., *Acoustic An Introduction*. Taylor & Francis, 2006.
[33] Chaigne A. and Kergomard J., *Acoustics of Musical Instruments*. Springer Verlag New York, 2016.
[34] Kim Y. H., *Sound Propagation: An Impedance Based Approach*. 2010.
[35] Bruneau M., Garing C., and Leblond H., Quality factor and boundary-layer of lower order modes in acoustic cavities, *J. Phys. 46*, vol. 46, pp. 1079–1085, 1985.
[36] Gupta A. K. and Tiwari A., Transfer Matrix Method for Noise Attenuation on Single Expansion Chamber Muffler having Central Inlet and Central Outlet with Experimental Techniques and FEA Validation, *Int. J. Theor. Appl. Sci.*, vol. 7, no. 2, pp. 14–20, 2015.
[37] Haupt R. L. and Haupt S. E., *Practical genetic algorithms*. 2004.
[38] Chipperfield A. J. and Fleming P. J., MATLAB Genetic algorithm toolbox, *IEE Colloq.*, no. 14, 1995.
[39] McCall J., Genetic algorithms for modelling and optimisation, *J. Comput. Appl. Math.*, vol. 184, no. 1, pp. 205–222, 2005.
[40] Bramantyo N., Desain Resonator Hemlholtz Ganda dengan Menggunakan Matlab, Universitas Sebelas Maret, 2006.
[41] Samanta S., Genetic Algorithm : An Approach for Optimization (Using MATLAB), *Int. J. Latest Trends Eng. Technol.*, vol. 3, no. 3, pp. 261–267, 2014.
[42] Imran M., Khan R., and Badshah S., Investigating the effect of delamination size, stacking sequences and boundary conditions on the vibration properties of carbon fiber reinforced polymer composite, *Mater. Res.*, vol. 22, no. 2, 2019.